Perfectly Understood Non-Uniformity: Methods of Measurement and Uncertainty of Uniform Sources

Joe Jablonski, Dan Scharpf, Saurabh Rabade, Luke Dobrowski, Chris Durell, Jeff Holt
Labsphere, Inc., 231 Shaker Street, North Sutton, NH 03260

ABSTRACT

Uniformity from Lambertian optical sources such as integrating spheres is often trusted as absolute at levels of 98% (+/- 1%) or greater levels. In the progression of today's sensors and imaging system technology that 98% uniformity level is good, but not good enough to truly optimize pixel-to-pixel and sensor image response. The demands from industry are often for "perfect" uniformity (100%) which is not physically possible, however, *perfectly understood* non-uniformity is possible. A barrier to this concept is that the definition and measurement equipment of uniformity measurements often need to be very specific to the optical prescription of the unit under test. Additionally, the resulting data are often a relativistic data set, assigned to an arbitrary reference, but not actually given an expression of uncertainty with a coverage factor. This paper discusses several optical measurement methods and numerical methods that can be used to quantify and express uniformity so that it has meaning to the optical systems that will be tested, and ultimately, that can be related to the Guide to the Expression of Uncertainty in Measurement (GUM) to provide an estimated uncertainty. The resulting measurements can then be used to realize very accurate flat field image corrections and sensor characterizations.

Keywords: Remote Sensing, Uniformity, Uncertainty, Uniform Source, Image Sensors, Flat Field, FPN, Camera Calibration

1. INTRODUCTION

A radiometric imaging device requires minimization of error to achieve the best performance possible. Image error will primarily come from a bias level, a dark current, and fixed pattern noise (FPN) in the imaging array. Additional error sources such as non-linearity, thermal effects, integration times, and optical imperfections may also contribute to the combined error in the image. The bias level and dark noise can be subtracted out after some preliminary measurements, but the FPN remains with the device and requires flat-fielding of the imager with a known, uniform field to compensate for the inherent differences in pixel-to-pixel response in the sensor, or photo-response non-uniformity, PRNU. This flat field correction however needs to be performed for the range of camera operating conditions, such as distance (focus), radiance level, integration time, viewing angle, filter settings, etc. to account for the changing PRNU. In addition, the source itself should be tuned to represent the spectral content of the desired measurement field.

The challenge is therefore to create a uniform radiance field (or irradiance filed for a bare sensor) that mimics the camera scene and to quantitatively characterize the radiant flux received at each pixel. Knowing the excitation at each pixel then allows a correction to be made to account for the PRNU. Several approaches are available for creating this uniform field such as back-illuminated diffusers[1][2], reflectance targets [3], and integrating spheres [4][5]. The use of an integrating sphere to create a Lambertian source will be addressed here.

Integrating sphere theory has been widely described to show analytically that a well-designed system can produce a highly-uniform radiance field[6]. A well-designed integrating sphere can deliver excellent uniformity as almost no other optical device can, but as with all real metrology devices, *it cannot deliver perfection.* Therefore, the discussion of perfection should begin at creating a situation of characterization where the method and means can deliver the realistic task of "perfectly understood non-uniformity". In this regard, some uniformity definitions may be more appropriate for a given application, but any definition that is explicitly defined, may be just as good as any other if it is characterized appropriately. All uniformity measurements are based on relativistic point measurements of the exit port of the sphere. To absolutely quantify uniformity, very specific definitions must be applied and be based on the optical parameters of the instrument to be tested. The end goal is to quantify the radiant flux received by every pixel in the sensor with a prescribed uncertainty.

1.1 Lambertian Sources

A Lambertian source is defined as one in which the radiance is constant with viewing angle. While the intensity is proportional to the cosine of the angle from the normal, the radiance is constant since the projected area varies with the cosine of the angle. The radiance of a Lambertian surface is constant and is also independent of the directional distribution of the incident illumination. Lambertian sources and surfaces are an idealized representation of the physical world. The light emitted from an integrating sphere and the light reflected from a diffuse reflective surface, such as Spectralon®, *approach* a Lambertian distribution, but do not perform exactly like the ideal case. It is this deviation from the ideal case that cause errors when the ideal assumption is made.

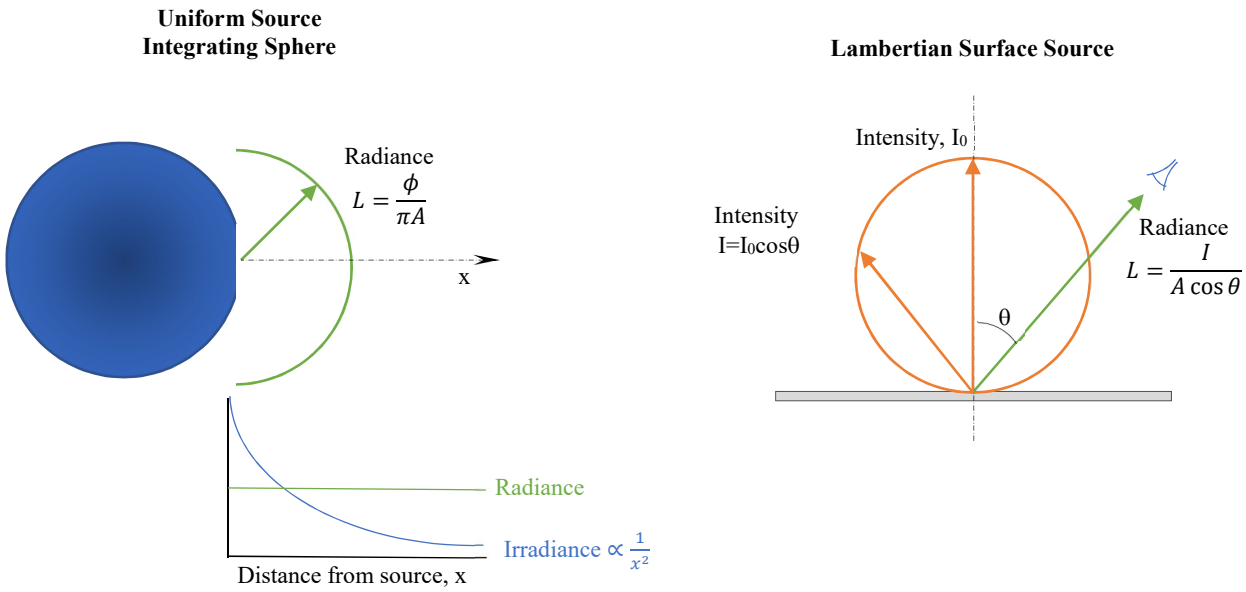

Figure 1 Lambertian Radiance distributions

1.2 Radiance Uniformity Prediction

Several approaches for numerically modeling the uniformity of an integrating sphere have been developed ranging from commercial ray-trace software to Monte Carlo Methods [8]-[10]. Advances in computing power have made some of these approaches tractable for simplified models and extracting trends based on design parameters; e.g., exit port diameter and coating reflectance. Prediction improvements may be made with actual coating BRDF measurements, but the computational requirements do not allow detailed designs to be evaluated for design tradeoffs.

1.3 Uniformity Definitions

Currently, there is no common method for defining the uniformity of the output from an integrating sphere. Whether the exit port is discretely mapped by a translating sensor, or in pixel space with a camera, the variation in the values at each point contribute to the uniformity of the source. Uniformity is typically calculated by normalizing each point to the mean, maximum, or value at the center of the source. The deviation in these normalized values is then used to describe the uniformity and expressed as a percentage. It should be stressed that perfect uniformity will have a value of 100%. In some applications, a value for *non-uniformity* is used, where the ideal value is 0%. A series of definitions will be provided here and summarized for their pros/cons.

The radiance at each point will be represented by, L_i, the mean radiance as , $\bar{L}$, and the ratio as: $L_i' = \frac{L_i}{\bar{L}}$.

1.3.1 Max Deviation Method

This value provides a measure of the maximum deviation between any two locations across the plane of interest relative to the maximum value. For uniform source applications where uniformity is typically very high, this is a reasonable

definition because it provides a worst-case description of the output. This definition also provides a simple measure for comparison between systems. This method is independent of normalization since the normalizing factors cancel.

$$U_{Max\ Deviation} = \frac{L_{min}}{L_{max}} \quad (1)$$

1.3.2 Deviation Method

This value provides a measure of the deviation relative to the mean.

$$U_{Deviation} = \left[1 - \frac{L_{max} - L_{min}}{\bar{L}}\right] \quad (2)$$

If the values are normalized by the mean:

$$U_{Deviation} = [1 - (L'_{max} - L'_{min})] \quad (3)$$

1.3.3 Mean Deviation Method

Since the high or low deviation from the mean will be half of the difference between the maximum and minimum values, this difference is divided by 2 to indicate the uniformity based on the average deviation from the mean:

$$U_{Mean\ Deviation} = \left[1 - \frac{\left(\frac{L_{max} - L_{min}}{2}\right)}{\bar{L}}\right] \quad (4)$$

This can also be expressed as:

$$U_{Mean\ Deviation} = \left[1 - \frac{L'_{max} - L'_{min}}{2}\right] \quad (5)$$

1.3.4 Coefficient of Variation Method

The previous descriptions of uniformity utilize only two points in the entire source field. By calculating the standard deviation from all the points, a measure of the dispersion in the light field is obtained which can provide a better description of the overall uniformity.

$$s_L = \sqrt{\frac{1}{N}\sum_{i=1}^{N}(L_i - \bar{L})^2} \quad (6)$$

The CoV is defined as the ratio of the standard deviation to the mean. The uniformity can then be expressed as:

$$U_{COV} = \left[1 - \frac{s_L}{\bar{L}}\right] \quad (7)$$

Note that this expression for the standard deviation is equivalent to the nonuniformity term used in references [8] and [9].

1.3.5 Summary of Uniformity Definitions

A typical uniformity map is shown in Figure 2 for a 0.5m dia sphere with a 20.3cm exit port. Five sources were used on the sphere with a total of 710W and distributed as shown. The 150W lamp at the 12:00 position was outfitted with a turning mirror and a variable attenuator that traversed a computer-controlled blade in front of the light path to allow adjustability in the output radiance. Each lamp is also independently controlled to adjust output levels. The uniformity map shown is for the full-power condition. Note that there is a definite skew in the uniformity toward the side of the sphere with the dominant light sources. The various calculation methods provide differing values of uniformity shown in Table 1.

Table 1 Uniformity Calculations for 0.5m sphere.

Calculation Method	Uniformity
Max Deviation	97.2%
Deviation Method	97.1%
Mean Deviation	98.6%
CoV	99.3%

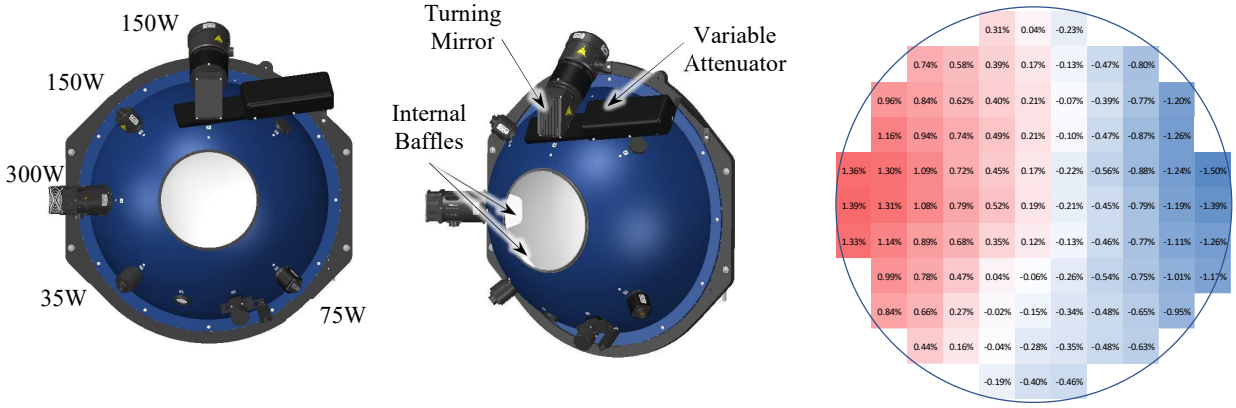

Figure 2 0.5m integrating sphere with 5 sources (710W) and the associated uniformity map.

A series of sample uniformity maps were created to illustrate how the calculation method represents the mapping in some extreme cases. The maximum deviation from the mean of 1.0 in each map is 2%. Similar uniformity values are calculated for very different maps, indicating that a numeric value can represent a wide range of possible radiance distributions. Without seeing the map, the uniformity value may be misleading, and will not provide all of the information required to make a decision about the appropriateness of the uniformity for a given application.

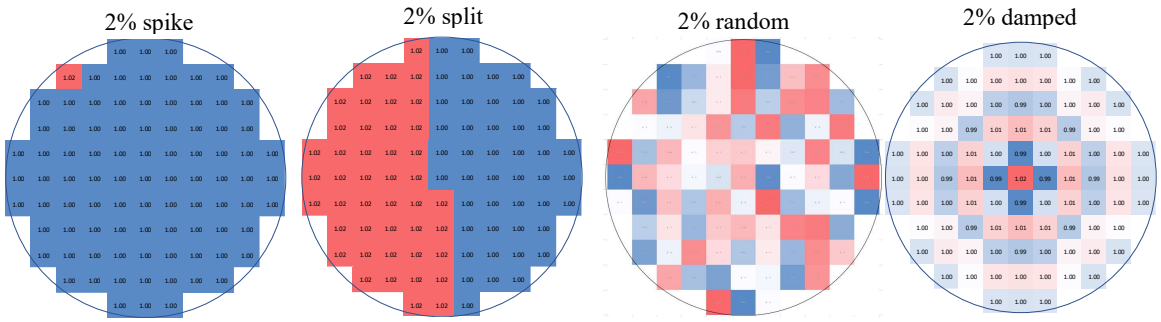

Max Dev.	98.0%	98.0%	98.1%	96.7%
Dev. Method	98.0%	98.0%	98.0%	96.7%
Mean Dev.	99.0%	99.0%	99.0%	98.3%
CoV	99.8%	99.0%	99.4%	99.5%

Figure 3 Uniformity calculations for various simulated uniformity maps.

2. MEASUREMENT METHODS

Measuring uniformity requires acquiring knowledge of light levels as a function of spatial position. This can be done with a point-by-point scanning method using a colorimeter or detector, or with an imagining device. To achieve absolute levels of radiance or irradiance, the measuring device requires calibration. For uniformity calculations, no calibration is required since the uniformity calculation results in a nondimensional value. In all cases, the point source, or the pixel representation requires the user to determine the corresponding physical area represented by each reported data point. The field of view of the sensor and the spatial resolution of the measurement will affect the reported uniformity. Because of the high contrast at the edge of the exit port of an integrating sphere, standard practice at Labsphere is to utilize 90% of the exit port diameter when calculating uniformity. In some cases, requests are made to calculate uniformity over smaller subsets of the exit port to achieve a more representative value for the portion of the field that will be used in the application with the DUT.

2.1 Discrete Spatial Mapping

By traversing a sensor across the exit plane of the integrating sphere, a map of discrete points is obtained that represent the emission field received by a sensor. This can be done with a bare sensor to achieve an irradiance map, or an imaging optic, or luminance meter to achieve a radiance map.

2.2 Mapping with Imaging Devices

A camera or imaging photometer may also be used to grab the entire emission field which eliminates many issues that can arise from sensor positioning and the duration of the discrete spatial mapping. This paper will focus on the use of the Westboro WP640 imaging colorimeter. This device is a 4.2 megapixel device with a 2048 x 2048 TE-cooled CCD array.

2.3 Flat Fielding for Uniformity Mapping

To utilize a camera as the uniformity measurement system, it needs to be flat-fielded prior to measuring a field for uniformity analysis to minimize the FPN. This process described in Figure 4.

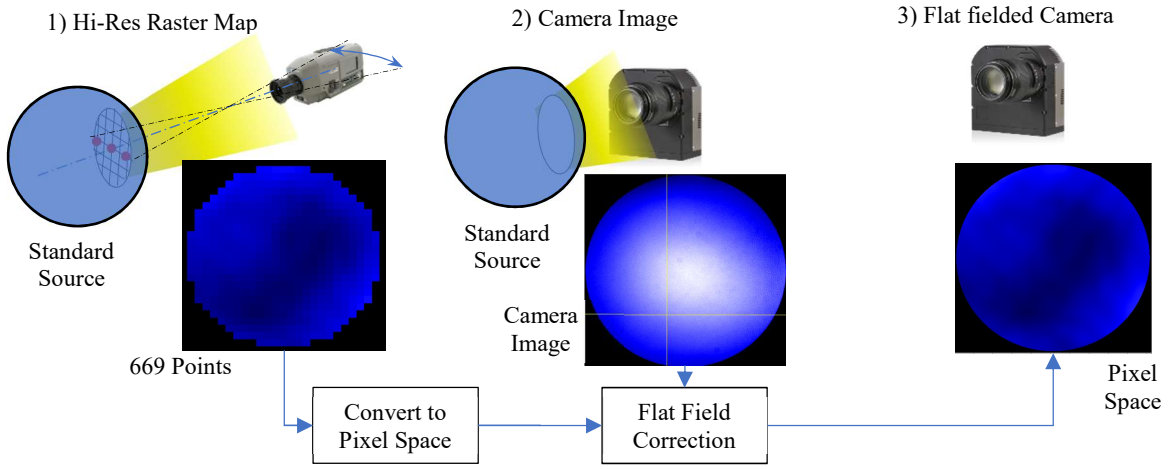

Figure 4 Uniformity calculations for various simulated uniformity maps.

To avoid edge effects, only 90% of the source diameter is utilized.

The raster scan utilizes a Konica Minolta CS-200 luminance meter that is mounted to a Universal Robotics UR5 robotic arm. The source for this purpose is a 20" diameter integrating sphere with four 50W quartz tungsten-halogen (QTH) lamps distributed evenly about the front hemisphere and an 8" dia. exit port. The multiple lamps in the system help to not only create a uniform field, but to also minimize temporal radiance fluctuations. A total of 669 points are recorded using an average of three measurements at each point with the CS-200 located at 31.8 cm from the exit port. Since the complete mapping requires 2 hours, there is potential for change in the source output over this period time. Decay of QTH lamps over this two-hour period is accounted for by normalizing the reading from the sphere detector monitor at each point in the map. Instead of traversing the CS-200 in a strict Cartesian plane parallel to the exit plane of the sphere, the CS-200 is positioned by modifying the yaw/pitch angles to represent the FOV of the camera that will be utilized in the next step. In this way, the map can be transformed to accurately represents the view of each pixel. The luminance meter is focused at the exit plane with a spot size of 1.3mm which corresponds to a 19mm spot on the back wall of the 20" sphere. A typical raster map of the source standard is shown in Figure 6. A detailed description of this procedure and examples of uniformity mapping can be found in Ref. [5].

The luminance at each point is normalized by the mean, and a bicubic spline interpolation is used to create the 2048 x 2048 values for mapping into angular camera pixel space. The data now represent the relative radiance received at each pixel. The WP640 camera then images the same standard source under the same conditions immediately following the raster map from the CS-200 luminance meter. The flat field map is created by dividing the raster map by the camera map and is specific to the camera setup including field of view, filter settings and integration time.

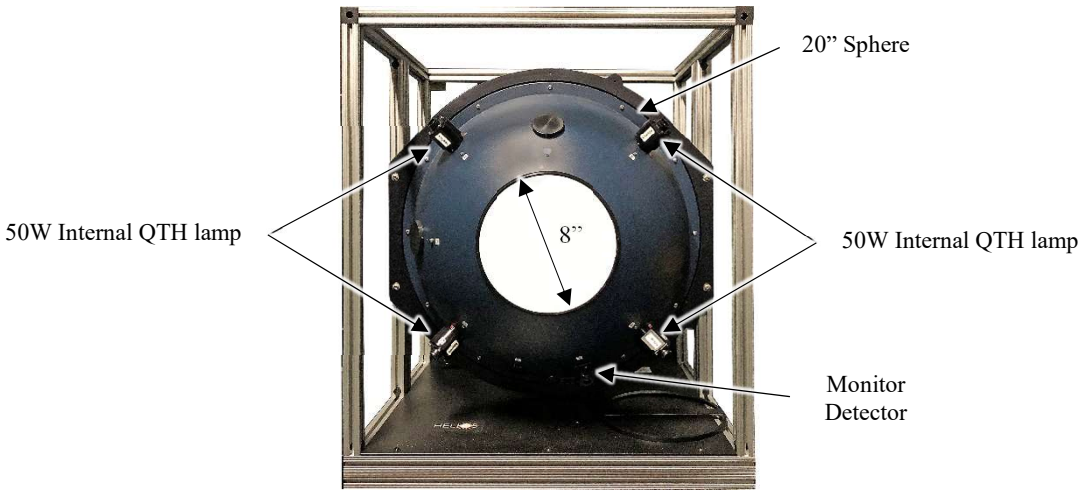

Figure 5 Geometry for Standard Source used in WP640 Camera Flatfield.

For measuring uniformity of a new source, this flat field correction is then applied to a camera capture of the new radiance field as shown in Figure 6. This corrected 2048 x 2048 map of the uniform source is then reduced to a more manageable grid spacing, typically 11 x 11, by vector analysis that captures the radiance projected into the new grid spacing. Uniformity is then calculated based on the values in the new grid spacing.

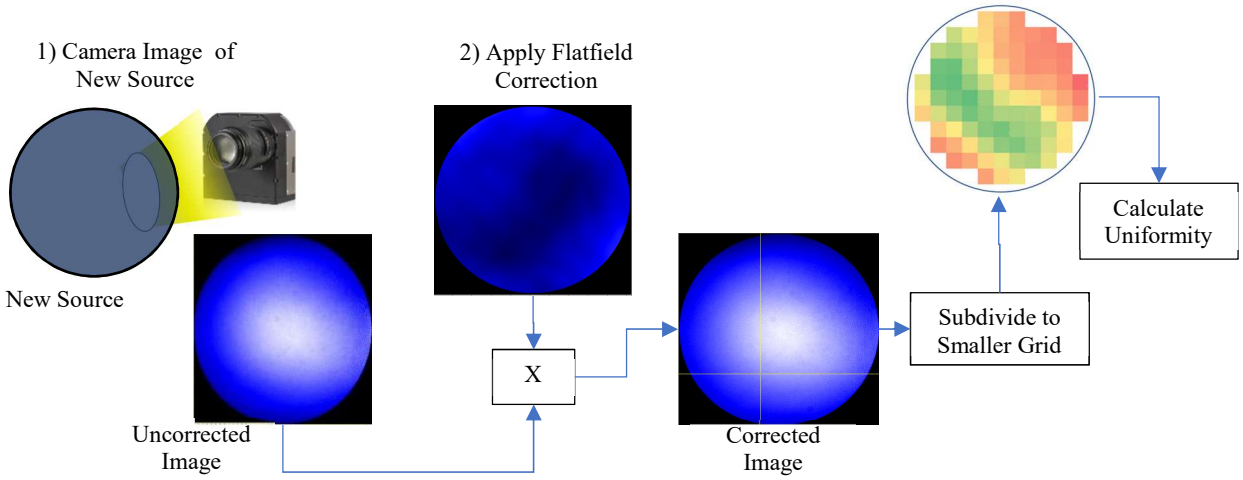

Figure 6 Uniformity Field for New Uniform Source.

3. UNCERTAINTY ESTIMATES

Estimating uncertainty of the measured uniformity of an integrating sphere utilizes the specific measurement equation for uniformity calculation. Many of the uniformity definitions only involve two points from the entire map which greatly simplifies the end calculation, but the propagation of uncertainty from the initial raster map of the standard source field, through the camera flat fielding and ultimately to the uniformity calculation can become quite complex and quickly becomes intractable for an explicit expression of uncertainty. Because of this, a Monte Carlo method (MCM) is applied that incorporates all the contributions and their associated correlations and nonlinearities. For any uncertainty analysis, an uncertainty propagation map can provide a description of all possible uncertainty contributions. These terms are then evaluated individually to assess the significance of their contribution. The propagation map for this uniformity process is shown below for the measurement of the uniformity of an integrating sphere source.

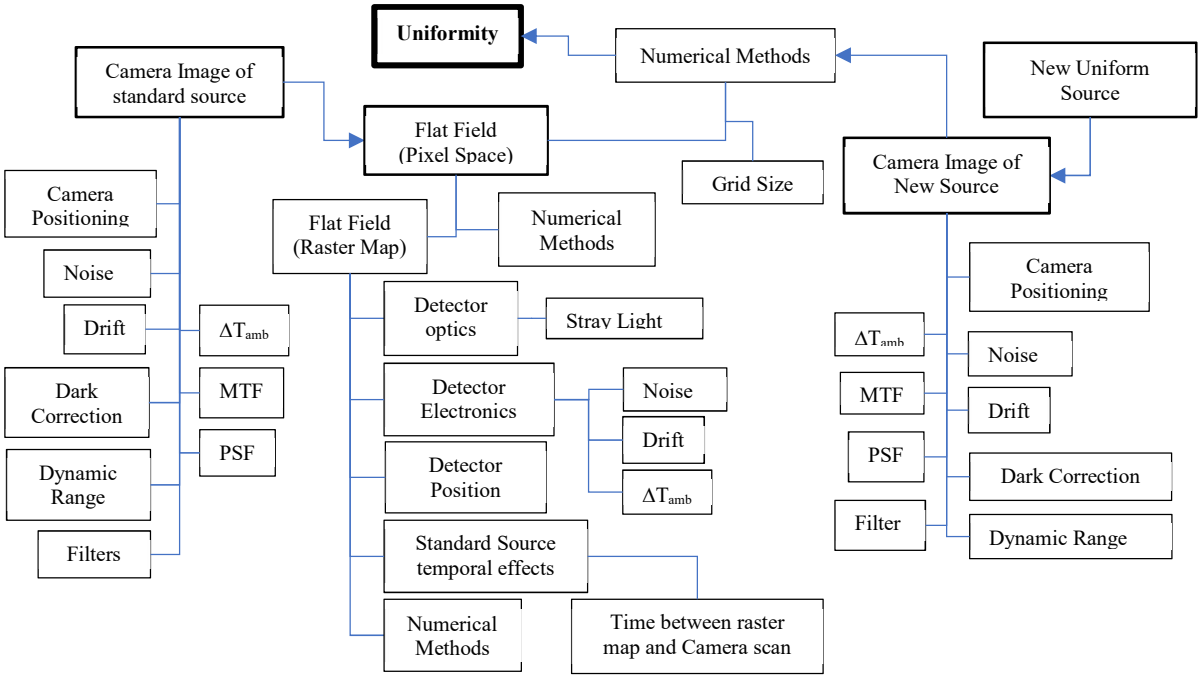

Figure 7 Uncertainty propagation map for uniformity calculation.

3.1 Flat Fielding Uncertainty Propagation

The measurement process for flat fielding a camera for uniformity measurements is shown below. Each step involves contributions to the uncertainty of the final camera flat-field which is propagated to any source that is subsequently measured for uniformity. As noted above in Figure 7, the uncertainty in the uniformity measurement would then also include effects of camera positioning, source effects, and the numerical methods used to create the desired uniformity grid size.

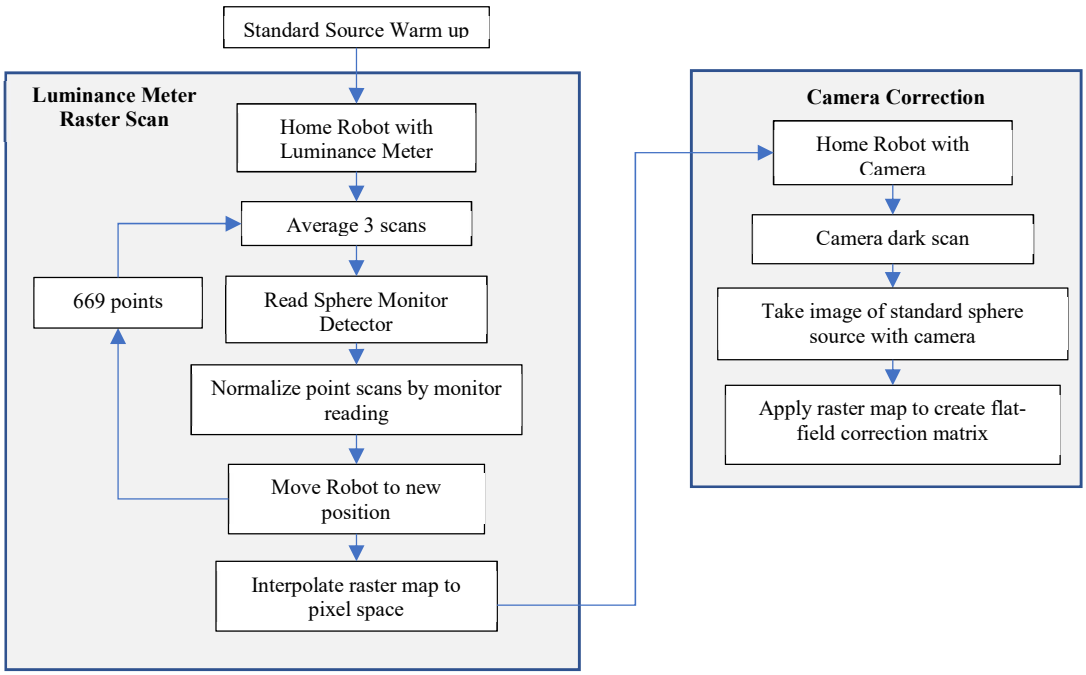

Figure 8 Flat-field process.

To determine the uncertainty in the flat field, the standard source was mapped 10 times with the luminance meter. This process provided the average values and standard deviations of the measurements at the 669 points in the map as shown in Figure 9. This dispersion in the data for each point included effects from the optical alignment, detector optics, electronics, detector positioning, and the source temporal effects. Since the measured values are all normalized by the mean, the systematic error from the instrumentation cancels in the analysis and the variability in the measurements at each point is what propagates through the MCM uncertainty analysis.

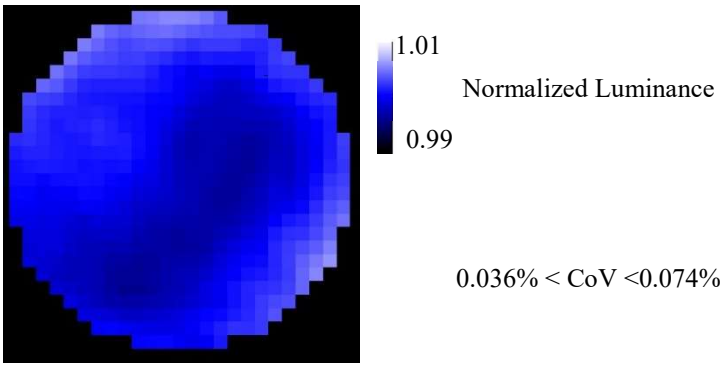

Figure 9 Normalized Luminance Raster map from CS-200 measurement of standard source

3.2 Camera Uncertainty Contributions

Since a normalized single camera image is used to create the map for calculating uniformity, only the relative error between pixels contributes to the uncertainty estimate in uniformity. For example, if the signal from all pixels increase by 1% due to thermal effects, then this effect would cancel when the pixel levels are normalized by the mean in the uniformity calculation. Therefore, only random error between pixels will contribute to the uniformity uncertainty.

Since uniformity is also being calculated for uniform sources, there are no edge effects and any error due to the modulation transfer function (MTF) or point spread function (PSF) of the camera are neglected.

The effect of noise in the measurement was determined by taking ten camera scans of the standard source and evaluating the standard deviation at each pixel. The accuracy of the WP640 camera is listed as ±4% for luminance (over 20 x20 pixels) and ±0.03% for short-term repeatability. The measured standard deviation at each pixel will include short term effects, noise and temporal variations in the source.

3.3 Explicit Uncertainty Estimates for Uniformity

Per the GUM [11] the propagation of uncertainty for a value, $y=f(x_1, x_2, \ldots x_N)$, can be described by the equation below which includes the correlated terms. The development of this equation however only takes the first term of the Taylor series expansion to estimate the uncertainty. In some cases, the nonlinear effects become important and must be included. The MCM includes both the correlation effects and any nonlinearities since the range of possible perturbations are successively propagated through the entire process that calculates the measurand.

$$u(y) = \sqrt{\sum_{i=1}^{N}\left(\frac{\partial f}{\partial x_i}\right)^2 u^2(x_i) + 2\sum_{i=1}^{N-1}\sum_{j=i+1}^{N}\frac{\partial f}{\partial x_i}\frac{\partial f}{\partial x_j}u(x_i,x_j)} \tag{8}$$

Applying Equation (8) to each of the uniformity definitions provides direct expressions of the combined uncertainty. The uncertainty in the uniformity for the Deviation Methods is:

$$u(Max.Dev.) = \sqrt{\left(\frac{1}{L_{max}}u_{L_{min}}\right)^2 + \left(\frac{-L_{min}}{L_{max}^2}u_{L_{max}}\right)^2} \tag{9}$$

$$u(Dev.) = \sqrt{\left(\frac{-1}{\bar{L}}u_{L_{max}}\right)^2 + \left(\frac{1}{\bar{L}}u_{L_{min}}\right)^2 + \left(\frac{L_{max}-L_{min}}{\bar{L}^2}u_{\bar{L}}\right)^2} \tag{10}$$

$$u(Mean.Dev.) = \sqrt{\left(\frac{-1}{2\bar{L}}u_{L_{max}}\right)^2 + \left(\frac{1}{2\bar{L}}u_{L_{min}}\right)^2 + \left(\frac{L_{max}-L_{min}}{2\bar{L}^2}u_{\bar{L}}\right)^2} \quad (11)$$

The uncertainty in calculated mean, $\bar{L}$, can be expressed explicitly for uncorrelated values as:

$$u(\bar{R}) = \frac{1}{N}\sqrt{\sum_{i=1}^{N} u^2(L_i)} \quad (uncorrelated) \quad (12)$$

The standard error, SE, of the calculated standard deviation, *s*, of a population can be written as:

$$SE(s) = \frac{s}{\sqrt{2N-1}} \quad (uncorrelated) \quad (13)$$

An explicit description of the uniformity uncertainty for the COV method can then be written with no correlated terms as:

$$u(CoV) = \sqrt{\left(\frac{1}{\bar{L}}\frac{s}{\sqrt{2N-1}}\right)^2 + \left(\frac{-s}{\bar{L}^2}\frac{1}{N}\sqrt{\sum_{i=1}^{N} u^2(L_i)}\right)^2} \, (uncorrelated) \quad (14)$$

Correlated effects in the uncertainty estimate for a uniformity measurement should not be ignored however, since variations in the source, thermal effects, cross-pixel talk, averaging, and the interpolation schemes, may all contribute to the expanded uncertainty.

Note also that the uncertainty for the individual luminance values (absolute or normalized) will each contain systematic errors that need to be included. The type A uncertainties can be estimated from multiple measurements for each spatial location, but the propagation of these uncertainties through the 2D interpolation schemes does not allow these explicit equations to be effective and therefore a Monte Carlo approach is utilized.

3.4 Monte Carlo Method for Uncertainty Estimates

Multiple measurements of the luminance from the CS-200 raster scans can be used to determine the mean, standard deviation, and probability distribution function at each point in the 669-point map. The Monte Carlo Method (MCM) then generates a random error based on these pdfs for each point as the data are propagated through the algorithm that creates the flat-field. Each time this process is repeated, a distribution of results is obtained for each pixel in the 2048 x 2048 flat-field map. When a sufficient number of cycles has been performed, each point will have its own distribution and associated uncertainty. This method will therefore include all correlations and nonlinear effects. In addition, any Type B uncertainties are also included by adding them in quadrature at each location in the raster scan.

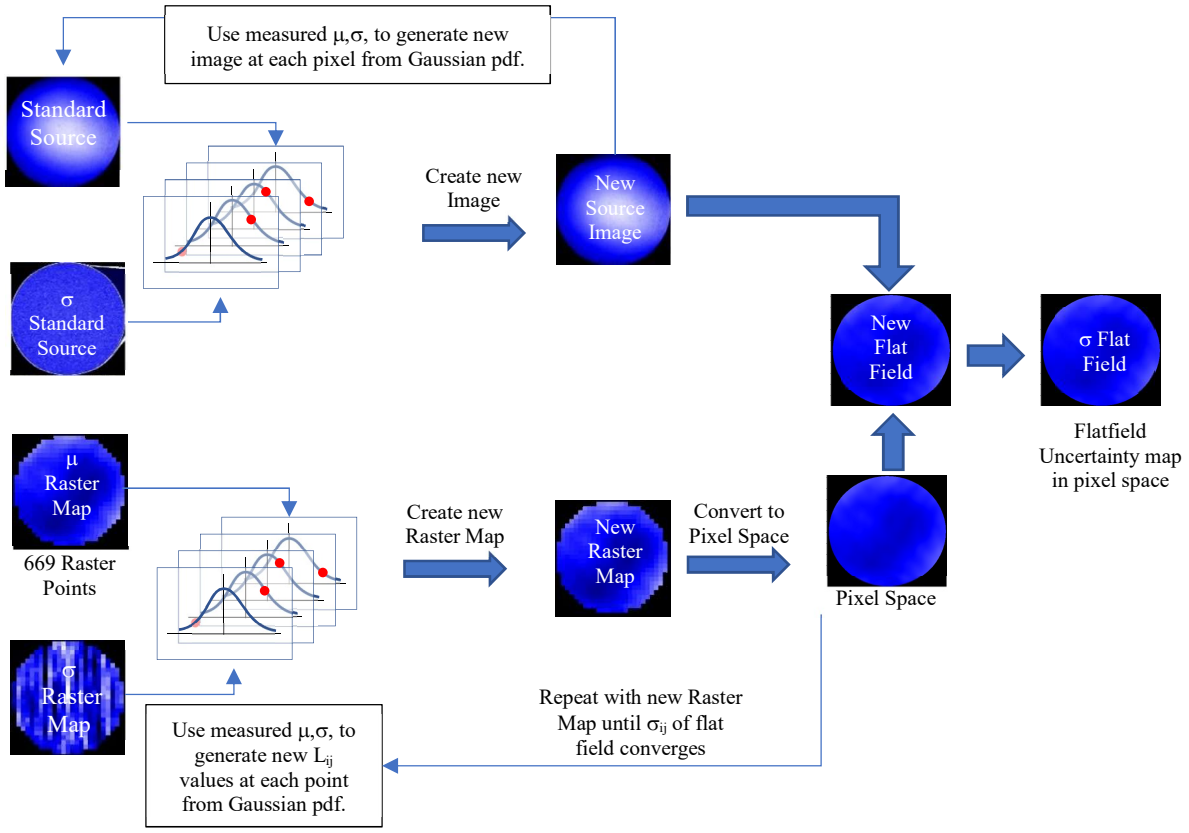

Figure 10 Monte Carlo process for estimating uncertainty in Flat Field correction map.

The output of the MCM was monitored by tracking the running standard deviation at four points in the map. As each successive iteration was included in the standard deviation calculation, the estimate of the standard deviation improved. Depending on the position of the monitor point, the level of variation was orders of magnitude different. The resulting map of radiance standard deviations is the uncertainty in the flat field correction map (k=1).

A map of uniformity is provided with a commercial uniform source and typically includes a spectral radiance calibration. In some cases, the simple knowledge of the uniformity is sufficient for future radiometric calibrations of imaging sensors. For the higher level of accuracies that are becoming ubiquitous, the uncertainty in the flatfield correction is propagated through the image correction of the uniform source. The numerical manipulations in this process necessitate using the MCM as outlined in Figure 12. This process is repeated until enough simulated variations are accumulated to produce a converged value of standard deviation of the calculated uniformity.

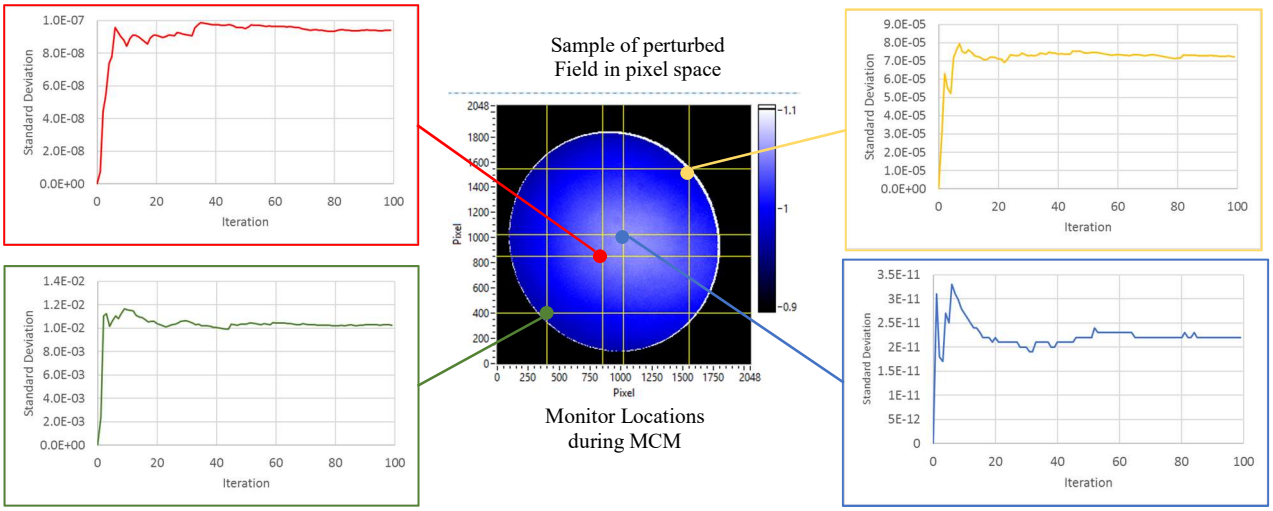

Figure 11 Monte Carlo process for estimating uncertainty in Flat Field correction map.

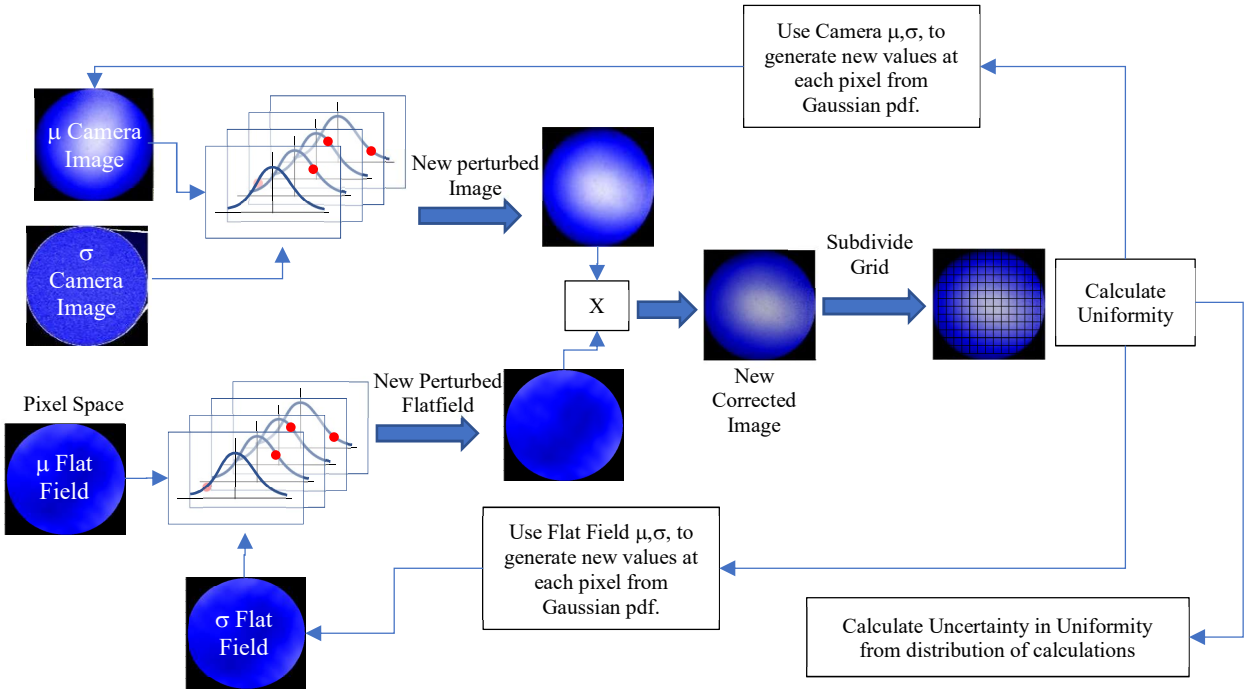

Figure 12 Monte Carlo process for estimating uncertainty in uniformity calculation from camera image.

The uncertainty convergence from the MCM process on a typical 20” uniform source is shown in Figure 13 when a final grid spacing of 11 x 11 is used. The source for these tests has a single 150W external QTH lamp and the variation in the estimated uncertainties converged at about 100 iterations. The expanded uncertainty estimates for the uniformity calculations are presented with a k=2 coverage factor are shown in Table 2 with units of %.

When the final grid spacing is increased to 25 x 25 points, the reported uniformity is worse than the 11 x 11 case as shown in Figure 14. With a smaller grid size, the variations in the pixel values are averaged into fewer boxes which subdues the extreme variations that ultimately leads to less dispersion in the uniformity calculations. This is apparent by the “hot spot” that appears in the 25 x 25 grid near the center which is not as predominant in the 11 x 11 grid. The uncertainty increases with higher grid spacing since the dispersion is now more pronounced in the radiance mapping at this higher resolution. As an example of this effect, the mean deviation method provides uniformity of 99.35% ± 0.034% and 98.97% ± 0.17%,

for the 11 x 11 and 25 x 25 grids, respectively. Understanding the requirements of the end application allows the user to correctly select the appropriate presentation of the uniformity data.

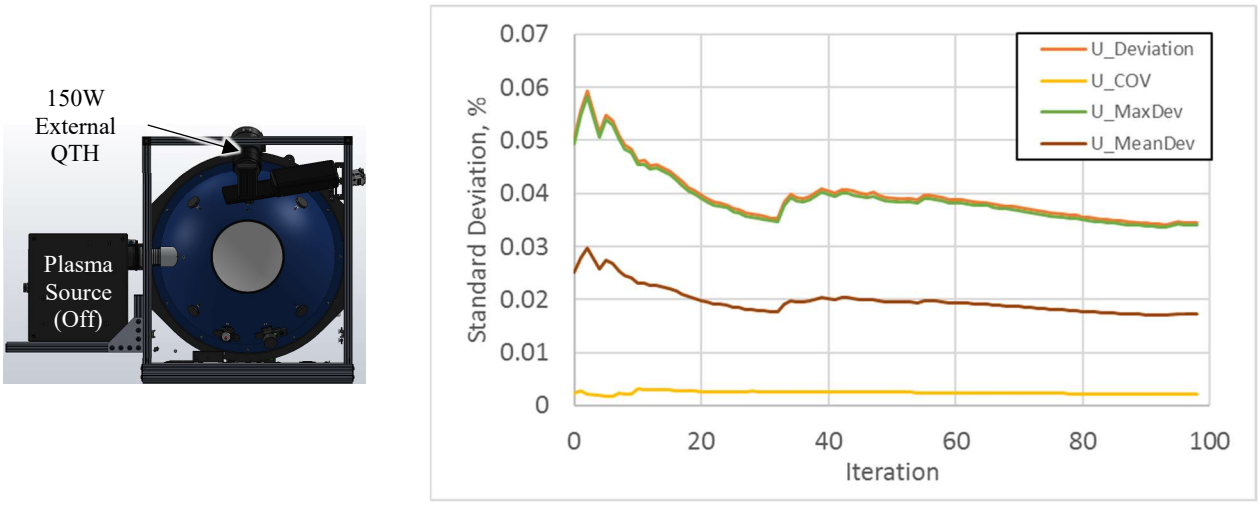

Figure 13 Running uniformity standard deviation from MCM uncertainty analysis for 20" test sphere and 11 x 11 grid spacing.

Table 2 Uniformity Uncertainty for 20" Test Sphere, one 150W lamp and 8" exit port.

	11 x 11 Grid		25 x 25 grid	
Calculation Method	**Uniformity**	**Expanded Uncertainty, k=2**	**Uniformity**	**Expanded Uncertainty, k=2**
Max Deviation	98.71%	±0.068%	98.0%	±0.32%
Deviation Method	98.71%	±0.069%	97.9%	±0.33%
Mean Deviation	99.35%	±0.034%	99.0%	±0.17%
CoV	99.687%	±0.0046%	99.667%	±0.0080%

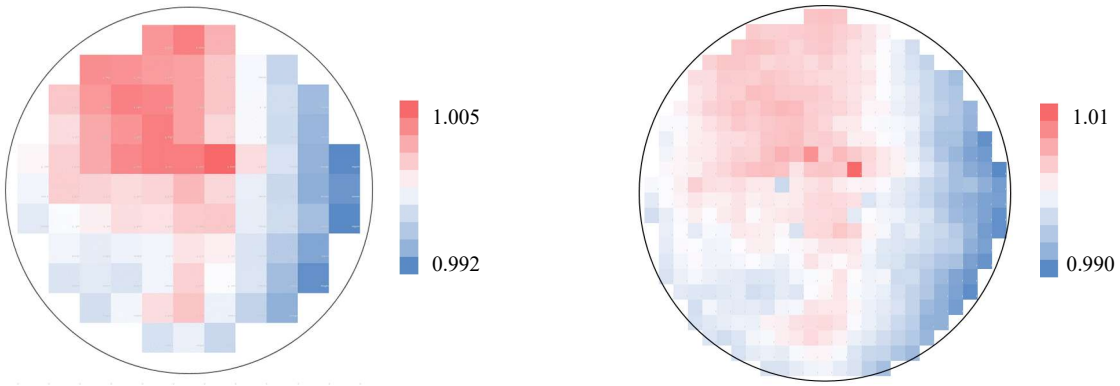

11 x 11 Grid 25 x 25 Grid

Figure 14 Uniformity Map for 20" test sphere at different grid spacings.

4. SUMMARY AND CONCLUSIONS

4.1 Conclusions

The demands for reduced uncertainty in radiometric calibrations is driving improvements in accuracy of calibration sources. For imaging applications this requires abandoning the assumption of perfect uniformity from an integrating sphere source and utilizing the spatial variation and the associated uncertainty. The MCM allows the Type A uncertainties to propagate through the complete calibration and measurement process while including the effects of correlation and numerical methods. Uncertainty in calculated uniformity has been shown to be dependent on the calculation method and grid spacing of the final map. Increasing the resolution of the final grid spacing reduces the calculated uniformity with an increase in uncertainty but provides better resolution for direct application of absolute radiance for correcting the image from the sensor. Characterizing and understanding the radiance distribution and the associated uncertainty is a critical step forward in reducing overall uncertainty of quantitative remote sensing image analysis.

4.2 Future Work

This process will continue to be refined and applied to a variety of different source types to assess the effects of more temporally varying sources, sphere configurations and grid spacing. It is important to understand that the uncertainty reported for a uniformity map (or any uncertainty) is an estimate of the uncertainty in the measured value at the time of the measurement. These values may be related to similar systems for making design and operating decisions, but a universal uncertainty value for a uniformity measurement process is not possible.

REFERENCES

[1] Ferrero, A., Lopez, M., Campos, J, and Sperling, A., "Spatial characterization of cameras for low-uncertainty radiometric measurements," Metrologia 51 316-325 (2014)

[2] Schulz, M, Buhr, E., Marholdt, K., Willemer, W., and Bergmann, D., "High-definition illuminated table for optical testing," Proc. SPIE 1400 529-538 (1999)

[3] Fox, N., Behnert, I., Pegrum-Browning, H., "A best practice guide to land "test-site" characterization QA4EO-WGCV-IVO-CLP-004," http://qa4eo.org/documentation.html

[4] McCorkel, J., McAndrew, B., Shuman, T., Zukowski, B., Traore, A., Rodriguez, W., Brown, S., and Woodward, J.., "Goddard Laser for Absolute Measurement of Radiance for Instrument Calibration in the Ultraviolet to Short Wave Infrared," CLEO, May 13-18, San Jose, CA (2018)

[5] Cariou, N., Durell, C., McKee, G., Wilks, D., and Glastre, W., "Effects of Lambertian sources design on uniformity and measurements," Proc. SPIE 9241, Sensors, Systems, and Next-Generation Satellites XVIII, 924116 (2014)

[6] Labsphere Technical Note, "A Guide to Integrating Sphere Theory and Applications," © 2017, Labsphere, Inc.

[7] Arecchi, A. V., Messadi, T., and Koshel, R. J., [Field Guide to Illumination], SPIE Field Guides, Volume FG II, SPIE Press, Bellingham, WA, p. 40 (2007)

[8] Prokhorov, A. V., and Hanssen, L. M., "Numerical modeling of an integrating sphere radiation source," Proc. of SPIE Vol. 4775, 106-118, (2002)

[9] He, Y., Li, P., Feng, G., Wang, Y., Zheng, C., Wu, H., and Sha, D., "Computer modeling of a large-area integrating sphere uniform radiation source for calibration of satellite remote sensors,"

[10] Lambda Research, TracePro Tutorial, "Integrating Sphere," (2011)

[11] JCGM 100:2008 GUM with minor corrections, "Evaluation of measurement data – Guide to the expression of uncertainty in measurement," First edition 2008, Corrected version , 2010.